JOURNAL OF MATERIALS SCIENCE 35 (2000) 2185–2192

Interaction of Ag ions with a vanadium pentoxide hydrate—Formation of silver vanadate at low temperature

S. KITTAKA*, Y. YATA, K. MATSUNO
Department of Chemistry, Faculty of Science, Okayama University of Science, 1-1 Ridaicho, Okayama 700-0005, Japan
E-mail: kittaka@chem.ous.ac.jp

H. NISHIDO
Institute of Natural Sciences, Okayama University of Science, 1-1 Ridaicho, Okayama 700-0005, Japan

Reactions between $V_2O_5 \cdot nH_2O$ sol and Ag^+ solution were investigated and new conventional reaction processes to produce silver vanadate bronzes were found. Reactions were surveyed as a function of the concentration ratios of Ag and V, and the reaction regions were divided into 4 parts dependent upon the reaction products. System 1: ion-exchanged sediment to produce β-$Ag_{0.35}V_2O_5$; System 2: needle-like α-$AgVO_3$ and hydrate to produce $Ag_{2-x}V_4O_{11}$ upon heating; System 3: new fine needle-like particle and small proportions of various dendrite crystallites; System 4: hydrate to produce β-$AgVO_3$ upon heating. The new needle-like particle of system 3 was analyzed by use of electron diffraction and XRD and found to be monoclinic, $a = 32.96$ Å, $b = 2.60$ Å, $c = 3.62$ Å, and $\beta = 91.88^\circ$. The material is named δ-$AgVO_3$. β-$Ag_{0.35}V_2O_5$ and $Ag_{2-x}V_4O_{11}$ were reversibly crystallized after melt. β-$AgVO_3$ was crystallized when the melt was cooled slowly, while α-$AgVO_3$ was crystallized when quenched rapidly.

1. Introduction

Vanadium pentoxide hydrate, $V_2O_5 \cdot nH_2O$, is an ionic layered compound [1, 2] and thus is a promising host for intercalation compounds which might carry new physico-chemical properties for dielectrics, catalysts, adsorbents etc. Various metal ions and polar molecules can be introduced between the layers through intercalation and/or cation-exchange reactions [3, 4, 5]. Its cation exchange capacities are about 0.32 : 0.16 : 0.1 mol per 1 mol V_2O_5 for the ions carrying the charges 1, 2, and 3. The reactions involved in these systems were found to be reversible except for the following cases [5]. Further reactions were observed after ion-exchange reaction with ions K^+, Rb^+, and Cs^+ when these ions were introduced in excess, by which orange-colored crystalline particles of $K_2V_6O_{16}$, $Rb_2V_6O_{16}$, and $Cs_2V_6O_{16}$ were formed, respectively. Besides these reactions, there have not been studies working with the reactions between $V_2O_5 \cdot nH_2O$ and metal ions which produce new vanadium bronzes. The present authors continue the study on the reactivity of the $V_2O_5 \cdot nH_2O$ against various chemical species to find new reaction processes.

Many vanadium oxide bronzes including Ag have been produced by solid state reactions, which vary in Ag, V, and O compositions [6–8]. However, the crystal structure analysis of this system is still an important subject to be studied [9–11]. Most of the products were formed by heating the mixture of component metal oxides and/or salts. Although this method is convenient for us to adjust the composition of metal ions we want to produce, it takes a long time to mix the component ions homogeneously, and oxygen content can not be controlled definitely. Znaidi *et al.* reported a new method starting with $V_2O_5 \cdot nH_2O$ to form $Ag_{0.35}V_2O_5$ in which a definite amount of Ag^+ was intercalated [12]. In this process, heat treatment of the material is required to reach the final product. However, an important benefit of this method is that mechanical mixing of the component substances is not required.

This report studies the formation of silver vanadates through the reactions of $V_2O_5 \cdot nH_2O$ with Ag^+ in a wet system at room temperature. A formation phase diagram with $V_2O_5 \cdot nH_2O$ sol and Ag^+ was drawn. The techniques used in the study were XRD, TG-DTA, TEM, SEM, and EPMA.

2. Experimental procedure

2.1. Chemical reactions

Raw material, $V_2O_5 \cdot nH_2O$, was prepared as a vanadium pentoxide sol by conventional cation-exchange-polymerization of ammonium metha-vanadate solution. The sol prepared was mixed with $AgNO_3$

* Author to whom all correspondence should be addressed.

0022–2461

solutions at varying ratios and maintained in the dark at room temperature (25–28°C) and 50°C. Here the indicated ionic concentrations of the systems are all for the systems after mixing. PH values of the mixtures studied were in rather narrow range around at 1.8–3 and were not controlled to avoid contamination of ions other than the reaction components. Atomic compositions of the precipitates produced were determined by EPMA (JEOL JXA-8900R). For comparison, the solid reaction products between Ag_2O and V_2O_5 powders were tested.

2.2. Crystal structure and texture analyses

The crystal structure of the formed materials were analyzed by powder X-ray diffraction (XRD); the apparatus used was Rigaku RAD-2R equipped with a Cu X-ray tube ($\lambda = 1.5418$ Å). For structure analysis of the crystals, reflection and transmission mode experiments were conducted on samples that oriented their crystal plane parallel to the flat plate. For the latter mode experiment, a sample was spread over an exfoliated thin mica plate and the spacing of the divergence slit used was 0.05 mm. For reflection mode measurements, it was 0.5 mm. The textures and crystal habits of the solids were studied by both a scanning electron microscope (SEM: JEOL JSM-5300LV) and a transmission electron microscope (TEM: HITACHI H8100). Selected area electron diffraction was observed for the structure analysis of the samples. The electron microscope was operated by using a 200 keV electron beam. Samples were heat-treated in air and quenched in an ice-water mixture. Significant differences were not found by changing the atmosphere with pure O_2.

2.3. Thermal analysis of the materials

Thermal properties of the solids (100 mg) were studied by TG-DTA measurements (ULVAC TGD-7000) in air at the heating rate of 5°C min^{-1}.

3. Results and discussion

Interaction of Ag^+ with $V_2O_5{\cdot}nH_2O$ was started with the colloid chemical point of view. The critical flocculation concentration (c.f.c.) was determined spectroscopically by measuring the turbidity of the sol with Ag^+. The determined value of 1.7 mmol dm^{-3} is much smaller than those for other monovalent ions like Li^+ (87 mmol dm^{-3}), Na^+ (17 mmol dm^{-3}), K^+ (7.6 mmol dm^{-3}), Rb^+(4.0 mmol dm^{-3}), and Cs^+ (4.5 mmol dm^{-3}). It has been understood that intercalation of ions plays a crucial role in the flocculation process of layered colloidal particles. The reason is that interlayer spacing is decreased to give dense structure without changing the structure of the *a-b* plane by intercalating the metal ions. However, the latter three ions gave their vanadates when the mixture was aged for a long time, suggesting that intercalated ions react with the host $V_2O_5{\cdot}nH_2O$. This fact leads us to expect that Ag^+ reacts with $V_2O_5{\cdot}nH_2O$ more strongly than with the above three alkaline ions, which was the case here. The XRD measurements of the sediments produced with Ag^+ just above c.f.c. indicated that materials other than the simple layered substance were formed; some Ag-V compounds were formed in this mixed system.

However, according to Znaidi *et al.* [12] and Bouhaouss *et al.* [13] Ag^+ is intercalated simply between the layers without reaction. Thus it is necessary to note the stability of the layered structure of $V_2O_5{\cdot}nH_2O$ against intercalation of Ag^+. At first, as has been done conventionally in the intercalation experiments of $V_2O_5{\cdot}nH_2O$, a film was formed on a glass plate and dried in air. The sample plate was wetted with $AgNO_3$ solution so that reaction equilibrium was attained. A marked difference was found in the chemical behavior from the solution systems. Interlayer distance was decreased as found in the intercalated substances, and more than 8 mmol dm^{-3} $AgNO_3$ were required to promote the chemical reaction to form the solid which was formed in the solution. This stable chemical property of the film might be explained by the marked crystallinity of $V_2O_5{\cdot}nH_2O$ when dried slowly. The comparative transmission mode XRD measurements were done on intrinsic samples, one of which was dried in air on a mica surface and an other was freeze dried. Sharper diffraction peaks (smaller line broadening) were found in the former. This kind of hard $V_2O_5{\cdot}nH_2O$ structure was also observed when H_2O vapor was adsorbed in the interlayer spacings [14]. Interlayer space did not expand by more than double the H_2O layers even under saturated H_2O vapor pressures, while wet gel is dried slowly on the glass plate, the interlayer distance decreased gradually from the larger one [15]. The present study is on the reactions in solution systems and those giving reaction products. It was found that the reaction varies, dependent upon the ratio of Ag^+ to $V_2O_5{\cdot}nH_2O$, so the whole the system was divided into 4 parts dependent upon the reaction products.

3.1. Reactions of Ag^+ with $V_2O_5{\cdot}nH_2O$

System 1. Mixing of $V_2O_5{\cdot}nH_2O$ sol with $AgNO_3$ solution brought about sedimentation of the solid, but the chemical reaction to produce the new phase was slow. In the system including a smaller amount of Ag^+, 0.05 mol(V^{5+})dm^{-3} /0.01 mol(Ag^+)dm^{-3}, for instance, structuring of the sediment required some time, as shown by the XRD pattern changes in Fig. 1a. This phase is named as System 1 whose concentration range is shown in the Fig. 3 phase diagram. The final product is visualized in Fig. 2a with less well-defined texture.

System 2. Fig. 1b shows the crystal growth in System-2, in which a well-defined crystalline phase (crystal-1) appeared from reddish brown precipitate formed by mixing the component solutions, 0.05 mol(V^{5+})dm^{-3}/0.1 mol(Ag^+)dm^{-3}. Needle-like crystallites were grown radially at some parts of the sediments, suggesting that the reaction starts at the surface of the hydrate and vanadate ions are supplied from the liquid phase. The reaction rate was increased at a higher reaction temperature (50 °C), but the phase relation was unchanged: a tiny crystalline solid appeared one day after mixing the component solutions. Finally this system

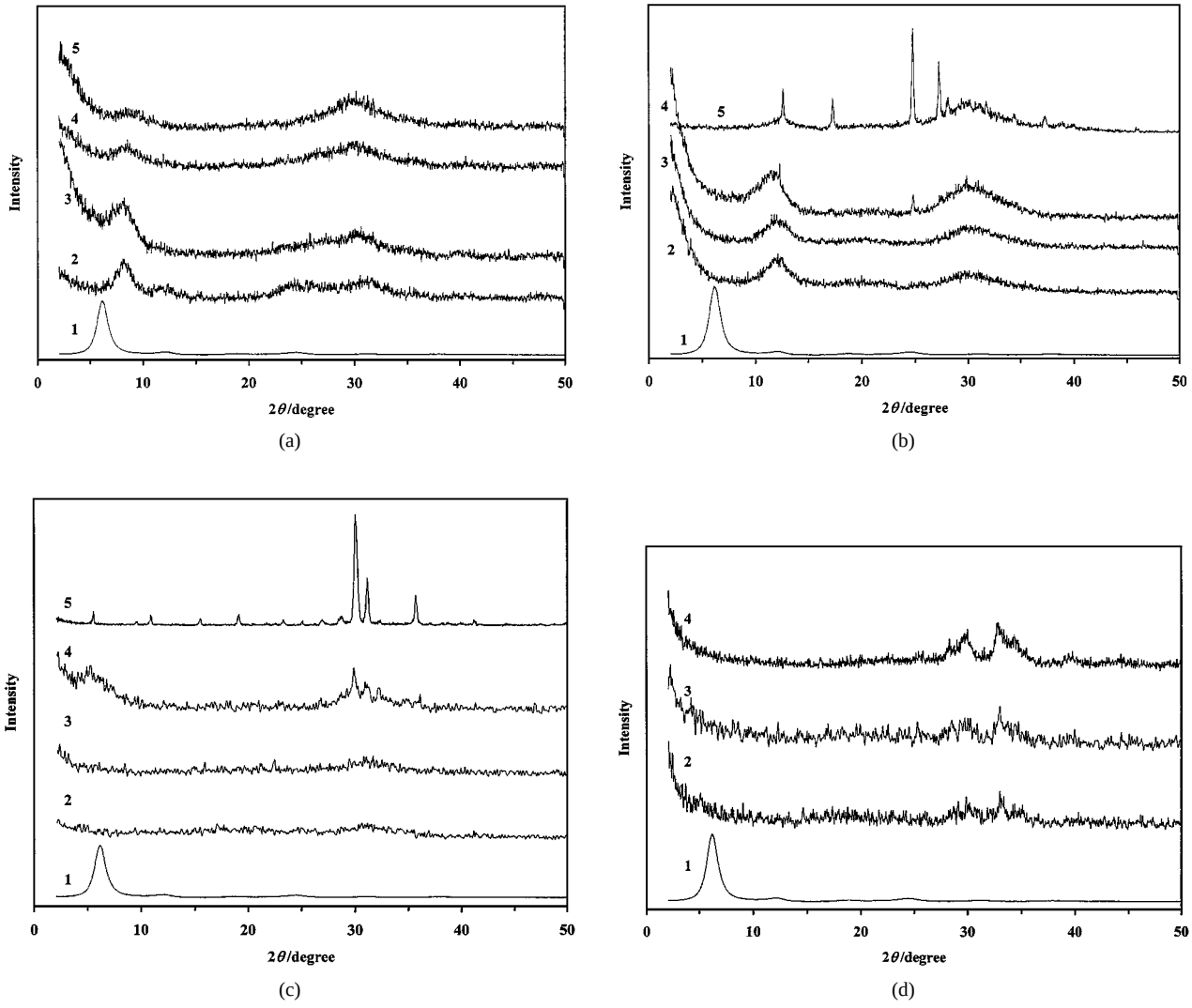

Figure 1 (a) XRD pattern changes of the system 1 with time: mixture of 0.05 (V^{5+}) mol dm^{-3}/0.01 (Ag^{+})mol dm^{-3}. 1. starting sample without Ag^{+}; 2, 1 h with Ag^{+}; 3, 1 day; 4, 2 weeks; 5, 1 month; (b) XRD pattern changes of the system 2 with time: mixture of 0.05 (V^{5+}) mol dm^{-3}/0.1 (Ag^{+})mol dm^{-3}. 1, starting sample without Ag^{+}; 2, 1 h with Ag^{+}; 3, 3 days; 4, 1 week; 5, 1 month; (c) XRD pattern changes of the system 3 with time: mixture of 0.01 (V^{5+}) mol dm^{-3}/0.1 (Ag^{+})mol dm^{-3}. 1, starting sample without Ag^{+}; 2, 1 day with Ag^{+}; 3, 1 week; 4, 2 weeks; 5, 3 months; (d) XRD pattern changes of the system 4 with time: mixture of 0.001 (V^{5+}) mol dm^{-3}/0.1 (Ag^{+})mol dm^{-3}. 1, starting sample without Ag^{+}; 2, 1 day; 3, 2 weeks; 4, 1 month.

was equilibrated as including two solid phases as can be seen in Fig. 2b. The crystal structure of the needle-like solid was newly analyzed by 4 circle XRD as α-$AgVO_3$ [16].

System 3. Fig. 1c shows the XRD patterns for the sediment obtained in the system, 0.01 mol(V^{5+})dm^{-3} /0.1 mol(Ag^{+})dm^{-3}, in which an ambiguous reddish brown hydrate is transfered into a crystalline phase with time (Fig. 2c). In this system, if the system is remained unstirred after mixing new bright orange-yellow crystalline phase appeared over the sediments. In the final state, all the hydrates disappeared and gave singly crystalline precipitate. Thus crystallization was conducted via solute species of vanadate ions. This is named temporarily as crystal-2 in the System-3.

System 4. Fig. 1d shows the rapid structuring of the sediment after mixing. The product should be fine β-$AgVO_3$ particles as shown below. However, the sediment was apparently just precipitated hydrate (Fig. 2d) and could not be visualized by electron microscope.

Fig. 3 is the phase diagram determined after equilibration in each system for more than 1 month. The concentrations of ions described are those included in the systems and not the equilibrated ones.

3.2. Phase properties of the sediments and crystals

System 1. An atomic ratio of Ag to V in the hydrate-1 was determined to be 0.34 : 2, which is close to the monovalent ion exchange capacity of $V_2O_5 \cdot nH_2O$ [5] and similar to that reported by Znaidi *et al.* [12]. Fig. 4-1 shows the DTA curve for the sample marked by the asterisk in Fig. 3. After a small peak which originates from dehydration, a sharp endothermic peak appeared at 541°C. A second run of the 600°C-heated sample did not give an endothermic peak at the same temperature. This indicates that some irreversible phase change has taken place at 541°C. The detailed analysis of XRD patterns of the sample heated at higher temperatures illustrates the appearance of the two phases, β-$Ag_{0.35}V_2O_5$ (probably β-$Ag_{0.35}V_2O_{5.17}$) and $Ag_{1.2-x}V_3O_8$, the latter of which is noted with the mark • in Fig. 5a: the formula employed for these substances are after Casalot

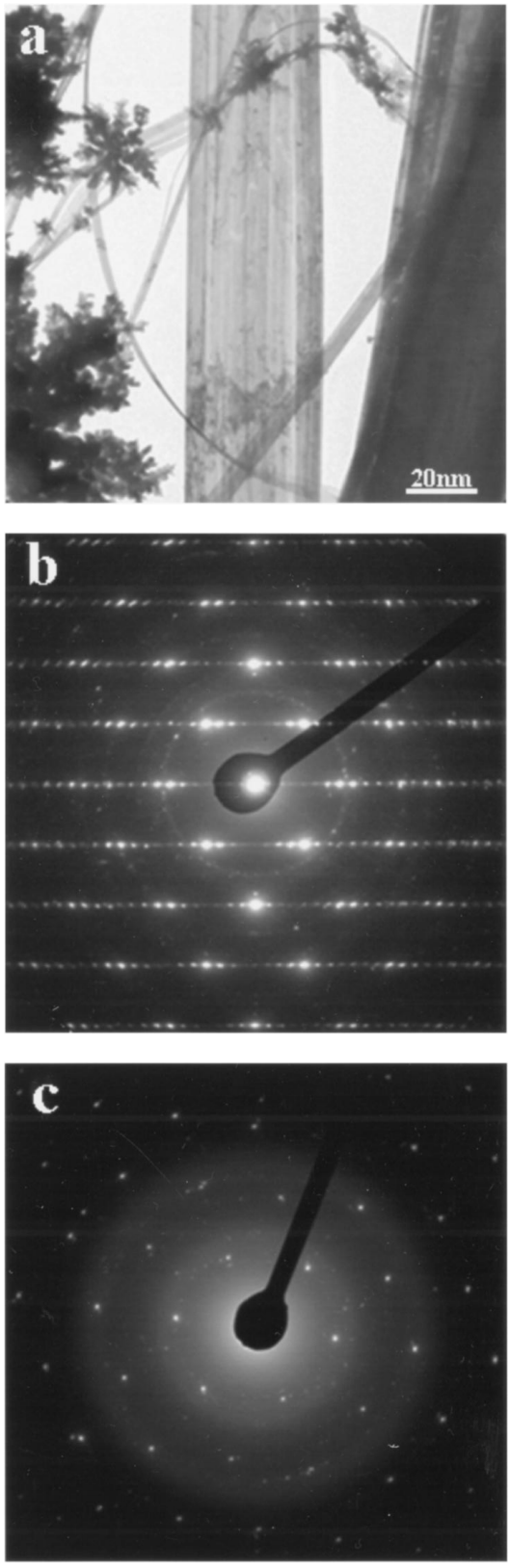

Figure 2 SEM photographs of the precipitates obtained by the reactions of varying ratios of $V_2O_5 \cdot nH_2O$ and $AgNO_3$. Materials observed were taken from the samples marked with asterisks in Fig. 3 and analyzed in all the experiments. (a) system 1; (b) system 2; (c) system 3; (d) system 4.

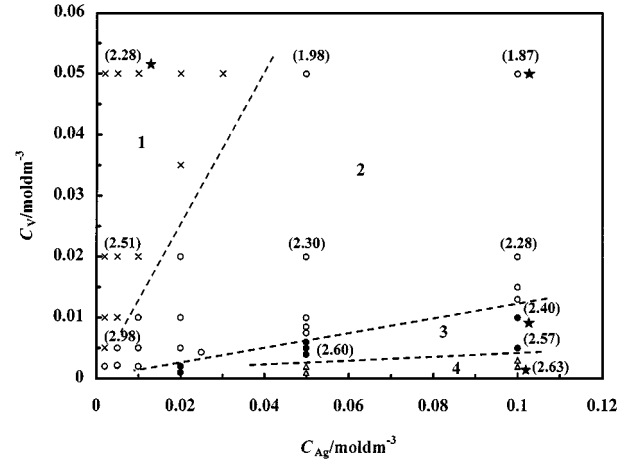

Figure 3 Formation phase diagram of the $V_2O_5 \cdot nH_2O$-$AgNO_3$ aqueous systems as presenting the characteristic sediments or crystalline particles, which is determined at room temperature. Numbers in the parenthesis indicate pH values of the system.

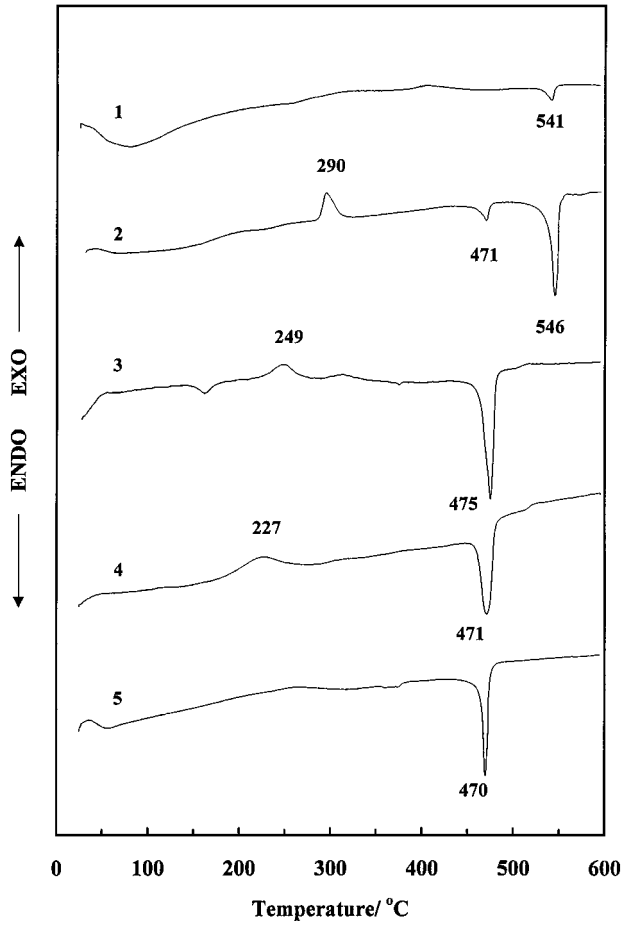

Figure 4 DTA curves of the sediments for the $V_2O_5 \cdot nH_2O$-$AgNO_3$ systems. The number in the left end of each curve is given for the sample: 1, hydrate 1 (system 1); 2, hydrate-2 (system 2); 3, crystal-1 (system 2); 4, crystal-2 (system 3); 5, hydrate 3 (system 4).

and Pouchard [7]. As a matter of fact, however, some of them are overlapped with those for the former. The sample heated above 500°C is simply β-$Ag_{0.35}V_2O_5$. These experimental facts signify that the endothermic peak at 541°C is due to the melting of both phases. We may say that the sediment is somewhat heterogeneous in Ag content to give two kinds of silver vanadate phases, although ion-exchangeable intercalation is the main process. If we want to form β-$Ag_{0.35}V_2O_5$ conventionally V_2O_5 and Ag_2O by solid reaction, the heating temperature must be raised higher than 580°C (not shown here). Even at such a high temperature many efforts such as repeated grinding are required to complete the solid reaction. We can then conclude that the

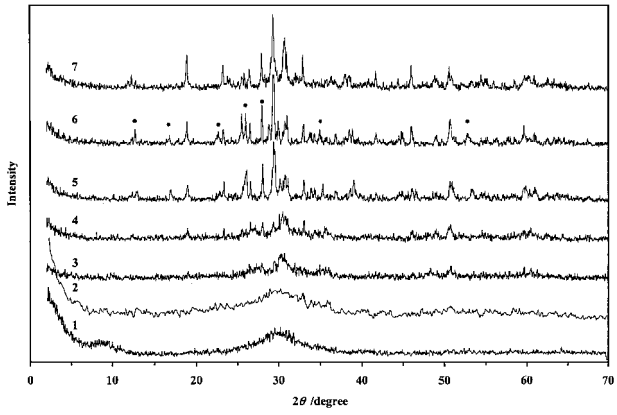

(a)

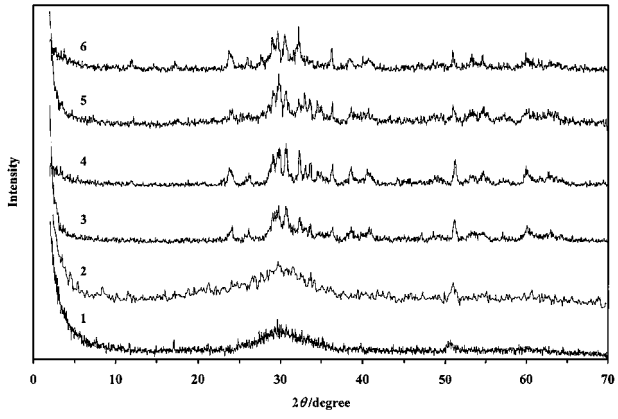

(b)

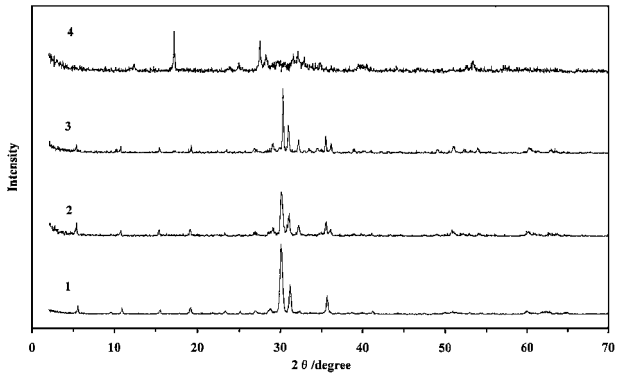

(c)

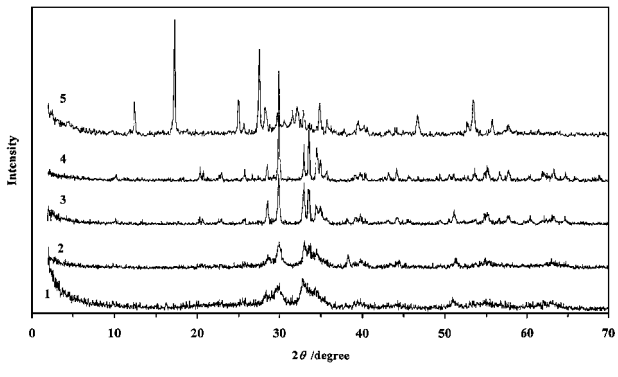

(d)

Figure 5 XRD patterns of the samples heated at increasing temperatures for 1 h. The number given for each peak at the left end of the curve indicates the temperature. Heating temperatures: (a) hydrate-1 (system-1); 1, 25°C; 2, 200°C; 3, 250°C; 4, 300°C; 5, 400°C; 6, 500°C; 7, 550°C. A mark • is for $Ag_{1.2-x}V_3O_8$; (b) hydrate-2 (system 2); 1, 25°C; 2, 250°C; 3, 300°C; 4, 400°C; 5, 500°C; 6, 550°C. (c) crystal-2 (system 3); 1, 25°C; 2, 200°C; 3, 450°C; 4, 500°C; (d) hydrate-3 (system 4); 1, 25°C; 2, 250°C; 3, 300°C; 4, 400°C.

homogeneous introduction of Ag^+ evenly, at least in the main part of interlayer spaces of $V_2O_5{\cdot}nH_2O$, provokes the chemical reaction to produce β-$Ag_{0.35}V_2O_5$ at a lower temperature.

System 2. This system is composed of two solid phases, a less well defined sediment (hydrate-2) and a needle-like crystal (crystal-1), as shown in Figs 1b and 2b. The details of the structure and thermal properties of crystal-1 were reported in the previous work [15]. It was defined as α-$AgVO_3$ with monoclinic structure C2/c(#15) and was ascertained to be exothermally transformed into β-$AgVO_3$ at 249 °C and molten at 475 °C.

DTA curve of the hydrate 2 is shown in Fig. 4. Clear peaks appear at 290, 471, and 546°C and have been analyzed in combination with the XRD data (Fig. 5b). We can understand that the sediment is crystallized at 290°C from almost amorphous matter into crystalline $Ag_{2-x}V_4O_{11}$ and has improved continuously its crystallinity up to 500°C. This signifies that Ag^+ should be homogeneously dispersed in a $V_2O_5{\cdot}nH_2O$ phase. The atomic composition of the hydrate was determined as $V : Ag = 1 : 0.50$ and supports the above crystallization of crystalline $Ag_{2-x}V_4O_{11}$ from the hydrate. Needle-like crystal-1 (α-$AgVO_3$) was grown by consuming the hydrate sediment and Ag^+ ions in the solution. In other words, hydrates are dissolved in the solution to react with Ag^+ ions and form a crystal in the solution. It is interesting to find that after picking out all the crystallites (crystal-1) from the system, crystal-1 was produced again by adding $AgNO_3$ solution in the system. We anticipate that there is a reaction from hydrate to crystal-1 accompanied by Ag^+ and H_2O.

$$Ag_2V_4O_{11} + 2Ag^+ + H_2O \rightarrow 4\alpha\text{-}AgVO_3 + 2H^+ \quad (1)$$

As can be anticipated by the DTA curve 3 for the crystal-1 in Fig. 4, which shows that needle-like particles are molten at 476°C, a rather clear endothermic peak on curve 2 at 470°C is ascribed to the melting of trace contaminant of the former. The reason for this is that the needle particles are too tiny to pick out by hand work. The large endothermic peak at 546°C is due to melting of the sample. The observed XRD pattern observed coincides completely with that of the phase, $Ag_{2-x}V_4O_{11}$, reported by Zandbergen *et al.* who obtained this sample by the solid reaction of Ag_2O and V_2O_5 [10]. Thus, the present wet method is convenient to produce this bronze at a much lower temperature if one takes the sample in the early stage of the reaction before the growth of the crystal 1 (Fig. 1b).

System 3: In this system the final solid product was mainly composed of fine needle-like particles (crystal-2) as seen in Figs 2c and 6a. However, fine dendrite type crystal cannot be dismissed in this product (Fig. 6a). The powder XRD pattern of this sample cannot be identified with any single or combination of Ag-V bronzes which have been reported so far. DTA and XRD measurements indicated that this phase is kept up to 471°C, which is somewhat lower than 475°C observed for α-$AgVO_3$. Judging from the much larger proportion of the needle particles in the system, this thermal property

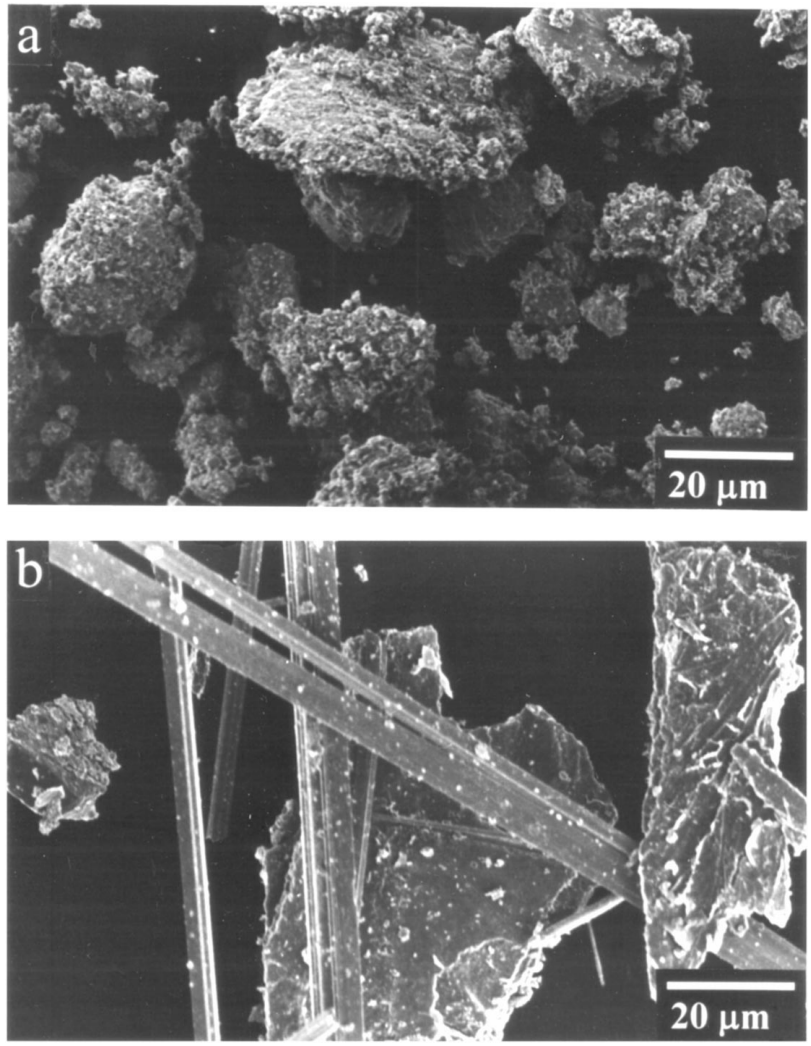

Figure 6 TEM photograph (a) of the sediment for system 3, in which the white bar indicates a measure of 0.1 μm and electron diffraction patterns of (b) a flat needle and (c) a dendrite particle, which were observed by introducing an electron beam normal to the particle plane. (*Continued*).

is due to the crystal-2. The chemical composition analysis indicates that this phase is one of the variables of $AgVO_3$ other than α-$AgVO_3$ and β-$AgVO_3$. This was substantiated by finding that the melt was crystallized into α-$AgVO_3$ when quenched in an ice-water mixture (Fig. 5d) and into β-$AgVO_3$ when cooled slowly. This is common behavior of $AgVO_3$ which has been known [16]. The crystal structure of the precipitates was examined by both XRD analyses in two modes (Fig. 7 (a) reflection and (b) transmission) and electron diffraction. Crystal-2 has a texture of flat needle-like particles and thus should give diffraction peaks for sequential single Miller indices changes in the reflection mode measurement. However, we can see two kinds of peaks in the pattern, i.e., small 3 sequential peaks at 9.47, 19.09, and 28.79°($d = 9.34$, 4.65, and 3.10 Å, respectively), and one strong peak at 30.07° ($d = 2.97$ Å). Then we can understand that there is another form of silver vanadate in the solid sample. The latter peak will be reasonably assigned to the diffraction by the main component by its size, crystal-2. Thus, the former group of peaks is due to the platelet fine dendrite particles shown in the left side of the picture (Fig. 6b).

The transmission mode XRD pattern of a single crystal should give the diffraction peaks assigned by combinations of the other two miller indices if the monoclinic crystal is placed on the substrate in parallel with one of the planes (Fig. 7b). The electron diffraction pattern of the crystal-2 shows the parallelogram pattern for the monoclinic structure (apparently face centered) when the electron beam is introduced normal to the flat particle plane (Fig. 6a). On the basis of these findings the least square fitting of XRD patterns from both reflection and transmission mode experiments was tried and the crystal parameters were $a = 32.96$ Å, $b = 2.60$ Å, $c = 3.62$ Å, and $\beta = 91.88°$. We give the name δ-$AgVO_3$ for the monoclinic silver vanadate (crystal 2). A density was determined by picnometry to be 4.22 g cm^{-3} which is smaller than 4.89 g cm^{-3} for α-$AgVO_3$ and 5.39 g cm^{-3} for β-$AgVO_3$. The efforts to analyze the crystal structure more definitely by using 4 circle XRD was not successful due to the small size of the specimen.

Electron diffraction patterns of the dendrite particles, which are observed normal to the particle planes, are varied from the particle to the particle of the sample. Here one example is shown in Fig. 6b. This is not correspondent with the finding of the single sequential diffraction peaks ($d = 9.34$ Å) in Fig. 7a. Then we may say here that chemical reaction is not equilibrated

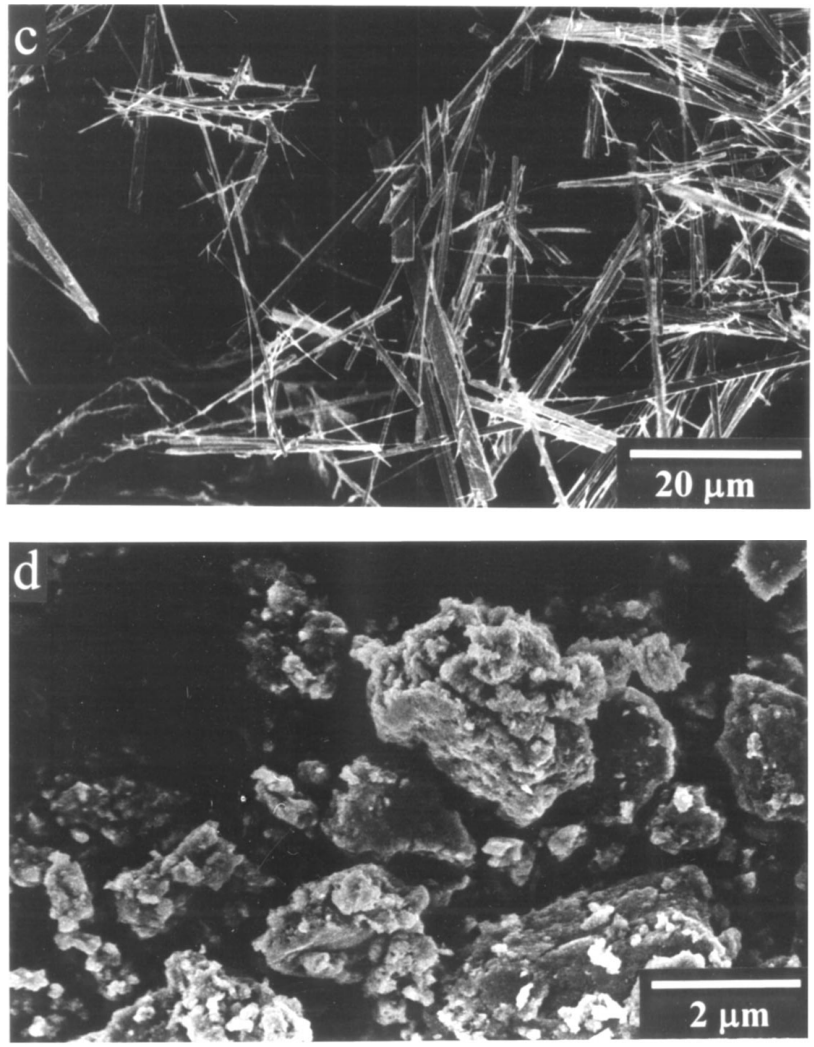

Figure 6 (*Continued*).

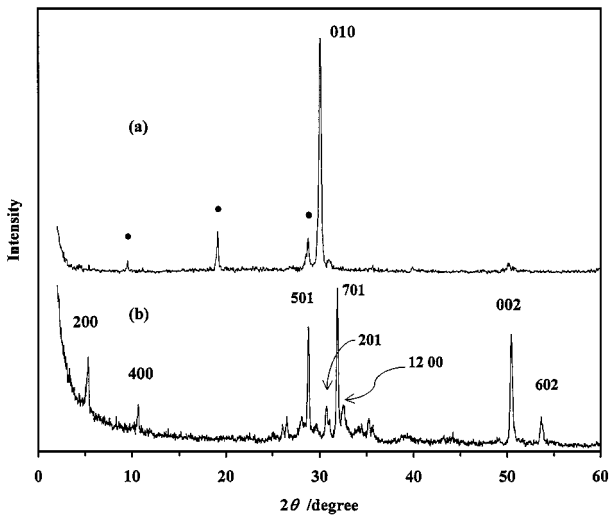

Figure 7 XRD patterns of the sediment for system 3 determined (a) in the reflection mode in which peaks marked with • are for the dendrite particles and (b) in the transmission mode.

after even more than one year, or a variety of phases are possible in this system. Thermal treatment of the system, however, at 50°C did not affect the solid structure, while hydrothermal treatment at 200°C for 24 h gave a small amount of β-$AgVO_3$ which might be the most stable phase allowing for the largest density among three $AgVO_3$ phases.

System 4. The material obtained in this Ag^+ rich system is a yellow sediment and its crystal structure may be assigned as β-$AgVO_3$, as shown by the XRD patterns which do not change up to the melting point (470°C) but are sharpened their peaks with increasing temperatures, markedly between 300 and 400°C. This is supported by the DTA curve of Fig. 4. Here again, when the melt is quenched in an ice-water mixture, it is solidified as α-$AgVO_3$. Then, the sediment carries a characteristic state different from the above crystal-1 and crystal-2, but shows similar behavior to that of the former. The most important finding in this system is concluded clearly that the β-$AgVO_3$ phase is quite easily formed at low temperatures without paying special effort to mixing the component metal oxides. This is compared with a solid state reaction at 420°C in which Ag_2O and V_2O_5 are mixed and heated [11].

4. Conclusions

A variety of reactions between $V_2O_5 \cdot nH_2O$ and Ag^+ were investigated in a wet system. The reactions proceed stepwise with increase in Ag^+ concentration and gave a reaction phase diagram.

(1) System 1: $V_2O_5 + 0.34Ag^+ + 0.34H_2O \rightarrow Ag_{0.34}V_2O_5(OH)_{0.34} + 0.34H^+$

(2) System 2: $2V_2O_5 + 2Ag^+ + H_2O \rightarrow Ag_2V_4O_{11} + 2H^+$

$Ag_2V_4O_{11} + 2Ag^+ + H_2O \rightarrow 4\alpha\text{-}AgVO_3 + 2H^+$

(3) System 3: $V_2O_5 + 2Ag^+ + H_2O \rightarrow 2\delta\text{-}AgVO_3 + 2H^+$

(4) System 4: $V_2O_5 + 2Ag^+ + H_2O \rightarrow 2\beta\text{-}AgVO_3 + 2H^+$

Three kinds of hydrates were precipitated in the reactions (1), (2), and (4) which afford $Ag_{0.34}V_2O_5$, $Ag_{2-x}V_4O_{11}$, and β-$AgVO_3$ upon heating, respectively. Two kinds of single crystalline needle-like particles were formed: α-$AgVO_3$ and a new δ-$AgVO_3$. It is proposed that reactions in the present systems are invoked by the less well-defined crystal structure together with the presence of water for the vanadium oxide hydrate to be dissolved to form intermediate chemical species, e.g., oligomers of polymerized vanadic acid, decavanadate ions, and VO_2^+ which can be main components in a diluted $V_2O_5 \cdot nH_2O$ sol [17]. Mechanisms of the reaction processes are now being studied in relation with the solute component in the systems.

Physico-chemical properties have been much less investigated on a series of $AgVO_3$ samples compared with other vanadium oxide systems and will be studied in the future study.

Acknowledgements

The authors express sincere thanks for financial support, and Special Grant for Cooperative Research administered by Japan Private School Promotion Foundation and Grant-in Aid for Exploratory Research 09874148, are also thanked. Miss Y. Kawada is also thanked for her assistance in experiments.

References

1. P. ALDEBERT, N. BAFFIER, N. GHARBI and J. LIVAGE, *Mat. Res. Bull.* **16** (1981) 669.
2. S. KITTAKA, M. SUMIDA and Y. KURODA, *Mat. Res. Soc. Symp.* **346** (1994) 697.
3. P. ALDEBERT, N. BAFFIER, N. GHARBI and J. LIVAGE, *Mat. Res. Bull.* **16** (1981) 949.
4. S. KITTAKA, H. YAMAMOTO, S. HIGUMA and T. SASAKI, *J. Chem. Soc. Faraday Trans.* **88** (1992) 715.
5. S. KITTAKA, N. UCHIDA, M. KATAYAMA, A. DOI and M. FUKUHARA, *Colloid Polym. Sci.* **269** (1991) 839.
6. B. RAVEAU, *Rev. chim. Mineral* **4** (1967) 729.
7. A. CASALOT and M. POUCHARD, *Bull. Soc. Chim. Fr.* (1967) 3817.
8. P. FLEURY and R. KOHLMULLER, *Compt Rend. Acad. Sci. Paris* **262** (1966) 475.
9. M. HA-EIERDANZ and U. MÜLLER, *Z. Anorg. Allg. Chem.* **619** (1993) 287.
10. H. W. ZANDBERGEN, A. M. CRESPI, P. M. SKARSTAD and J. F. VENTE, *J. Solid State Chem.* **110** (1994) 167.
11. P. ROZIER, J. M. SAVARIAULT and J. GALY, *ibid.* **122** (1996) 303.
12. L. ZNAIDI, N.BAFFIER and M. HUBER, *Mat. Res. Bull.* **25** (1990) 705.
13. A. BOUHAOUSS, P. ALDEBERT, N. BAFFIER and J. LIVAGE, *Rev. Chim. Miner.* **22** (1985) 417.
14. S. KITTAKA, Y. AYATSUKA, K. OHTANI and N. UCHIDA, *J. Chem. Soc., Faraday Trans.* I, **85** (1989) 3825.
15. S. KITTAKA, T. SUETSUGI, S. MORIKAWA and N. UCHIDA, *Langmuir* **9** (1993) 1104.
16. S. KITTAKA, K. MATSUNO and H. AKASHI, *J. Solid State Chem.* **142** (1999) 360.
17. J. LEMERLE, L. NÉJEM and J. LEFEBVRE, *J. Inorg. Nucl. Chem.* **43** (1981) 2683.

Received 25 May
and accepted 14 October 1999